PROCEEDINGS OF SCIENCE

QCD's equation of state from Dyson–Schwinger equations

Philipp Isserstedt,[a,b,†,*] **Christian S. Fischer**[a,b] **and Thorsten Steinert**[a,‡]

[a] *Institut für Theoretische Physik, Justus-Liebig-Universität Gießen, 35392 Gießen, Germany*
[b] *Helmholtz Forschungsakademie Hessen für FAIR (HFHF), GSI Helmholtzzentrum für Schwerionenforschung, Campus Gießen, 35392 Gießen, Germany*

E-mail: philipp.isserstedt@physik.uni-giessen.de, christian.fischer@theo.physik.uni-giessen.de, thorsten.steinert@dwd.de

In this contribution, we summarize a truncation-independent method to compute the equation of state within nonperturbative functional approaches. After demonstrating its viability, the method is applied to solutions obtained from a set of truncated Dyson–Schwinger equations for the quark and gluon propagators of (2 + 1)-flavor QCD to obtain thermodynamic quantities across the phase diagram of strong-interaction matter.

FAIR next generation scientists – 7th Edition Workshop (FAIRness2022)
23–27 May 2022
Paralia (Pieria, Greece)

[*] Speaker
[†] Present address: Frankfurt Consulting Engineers, Bessie-Coleman-Str. 7, 60549 Frankfurt am Main, Germany.
[‡] Present address: Deutscher Wetterdienst, Frankfurter Str. 135, 63067 Offenbach am Main, Germany.

PoS(FAIRness2022)024

1. Introduction

Both the experimental and theoretical exploration of the phase diagram of strong-interaction matter with its conjectured critical endpoint (CEP) is one of the leading research goals of contemporary high-energy physics [1–3]. The equation of state (EoS)—i.e., pressure, entropy density, and energy density—as a function of temperature and chemical potential holds the desired information to understand the various phases of QCD and is encoded in the thermodynamic potential.

The phase structure of QCD at vanishing chemical potential is well understood thanks to ab-initio lattice-QCD calculations [4, 5]. At nonzero chemical potential, however, these are severely hampered by the sign problem and complementary approaches are necessary. The nonperturbative functional framework of Dyson–Schwinger equations (DSEs) is well-suited for that, and significant progress has been achieved in recent years; see, e.g., Refs. [6–12] and Ref. [13] for a review.

Unfortunately, obtaining the EoS from DSEs is extremely difficult. Generally speaking, the starting point for the derivation of every DSE is the first derivative of the thermodynamic potential, and an integration is necessary to get hold of the potential itself. Alas, this integration is only possible for certain truncations. In this contribution, a truncation-independent method to compute thermodynamic quantities from DSEs is summarized that we put forward in Ref. [9].

2. Thermodynamics from the quark condensate

At nonzero temperature T and quark chemical potential μ, all thermodynamic information of QCD is encoded in its thermodynamic potential

$$\Omega(T,\mu) = -\frac{T}{V}\log\mathcal{Z}(T,\mu)\,, \tag{1}$$

where V is the volume of the system and $\mathcal{Z}$ denotes the grand-canonical partition function.[1] The EoS follows from standard thermodynamic relations [14]. For example, the pressure is given by $P(T,\mu) = -(\Omega(T,\mu) - \Omega(0,0))$ and the entropy density reads $s(T,\mu) = \partial P(T,\mu)/\partial T$.

Though in principle fixed, the current quark mass m can also be treated as an external, variable quantity: $\Omega = \Omega(T,\mu;m)$. In the action, it appears as the source for the quark-field bilinear $\overline{\psi}\psi$, and the quark condensate is thus given by $\langle\overline{\psi}\psi\rangle(T,\mu;m) = \partial\Omega(T,\mu;m)/\partial m$. This relation can be inverted, i.e., integrated with respect to the current quark mass, and allows us to express the difference of the thermodynamic potential evaluated at two arbitrary (unphysical) current quark masses m_1, m_2 (w.l.o.g., $m_1 < m_2$) as an integral over the quark condensate, viz.

$$\Omega(T,\mu,m_2) - \Omega(T,\mu,m_1) = \int_{m_1}^{m_2} \mathrm{d}m'\,\langle\overline{\psi}\psi\rangle(T,\mu;m')\,. \tag{2}$$

This equation is of little practical use because both Ω and $\langle\overline{\psi}\psi\rangle$ are divergent. The divergence is contained in the vacuum contribution to the thermodynamic potential, i.e., independent of temperature and chemical potential. Thus, a derivative of Eq. (2) with respect to T yields a divergence-free equation that relates the entropy density to the quark condensate according to

$$s(T,\mu;m_2) - s(T,\mu;m_1) = -\int_{m_1}^{m_2} \mathrm{d}m'\,\frac{\partial\langle\overline{\psi}\psi\rangle}{\partial T}(T,\mu;m')\,. \tag{3}$$

[1] For the sake of simplicity, here we consider only one (light) flavor.

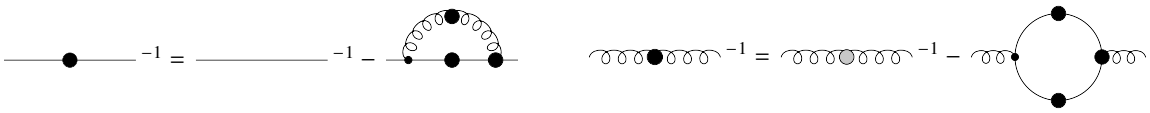

Figure 1: DSEs for the quark (left) and gluon (right) propagators. The former (latter) are denoted by solid (curly) lines while a large black dot indicates nonperturbative quantities. In the gluon DSE, the gray dot represents all diagrams with no explicit quark content. Feynman diagrams were drawn with JaxoDraw [16].

Finally, we set the lower integration limit to the physical current quark mass, $m_1 = m$, and send the upper one to infinity, $m_2 \to \infty$. An infinitely heavy quark becomes static and freezes out of the system, and the entropy density is then simply the one of pure-gluonic Yang–Mills gauge theory, $s(T, \mu; m_2 \to \infty) = s_{\text{gauge}}(T)$, which is known to a high precision from the lattice [15]. We thus arrive at

$$s(T, \mu) = s_{\text{gauge}}(T) + \int_m^\infty \mathrm{d}m' \, \frac{\partial \langle \overline{\psi}\psi \rangle}{\partial T}(T, \mu; m') \,, \tag{4}$$

which establishes a general relation between the entropy density and the quark condensate. We emphasize that Eq. (4) is obtained without any approximation and is therefore exact. Only the temperature derivative of the quark condensate as a function of the current quark mass (at fixed T and μ) is needed to compute the entropy density. This renders Eq. (4) quite general and not restricted to a specific approach, though it is particularly useful within the DSE framework where computing the thermodynamic potential is extremely difficult, while obtaining $\langle \overline{\psi}\psi \rangle(T, \mu; m)$ is straightforward.

3. Dyson–Schwinger equations

The quark condensate—sole input of Eq. (4)—is obtained from the nonperturbative quark propagator $S(T, \mu; m)$ through $\langle \overline{\psi}\psi \rangle(T, \mu; m) = \operatorname{Tr} S(T, \mu; m)$, where the trace is understood in the functional sense over flavor, color, Dirac, and momentum space d.o.f. We obtain S by solving a set of truncated DSEs that takes the backcoupling of quarks onto the gluon explicitly into account, which allows for a consistent mass and flavor dependence of all results. Equally important, the gluon becomes sensitive to the chiral dynamics of the quarks. This system has been studied extensively in other works (see, e.g., Refs. [6, 11, 13] and references therein) and predicts a second-order CEP at temperature $T_{\text{CEP}} \approx 119\,\text{MeV}$ and baryon chemical potential $\mu_{\text{B}}^{\text{CEP}} \approx 495\,\text{MeV}$.

In more detail, the nonperturbative quark and gluon propagators each obey a DSE that is shown diagrammatically in Fig. 1. Both contain higher-order correlation functions, e.g., the nonperturbative quark-gluon vertex, which satisfy their own DSEs. To cope with this infinite tower of coupled equations, we truncate as follows: (i) in the gluon DSE, all diagrams with no explicit quark content are replaced by fits to quenched, temperature-dependent lattice results; (ii) for the nonperturbative quark-gluon vertex, an ansatz is employed whose infrared dynamics are guided by a Slavnov–Taylor identity for the full vertex while its behavior in the ultraviolet is fixed by demanding the correct running of the propagators at large perturbative momentum scales. The quark-loop diagram is evaluated explicitly, thereby unquenching the gluon.

This system is solved numerically for $2 + 1$ flavors, which yields the nonperturbative quark and unquenched gluon propagators at arbitrary T and μ_{B}. For the sake of brevity, we refrain from showing explicit expressions and refer the reader to Refs. [6, 13] for details.

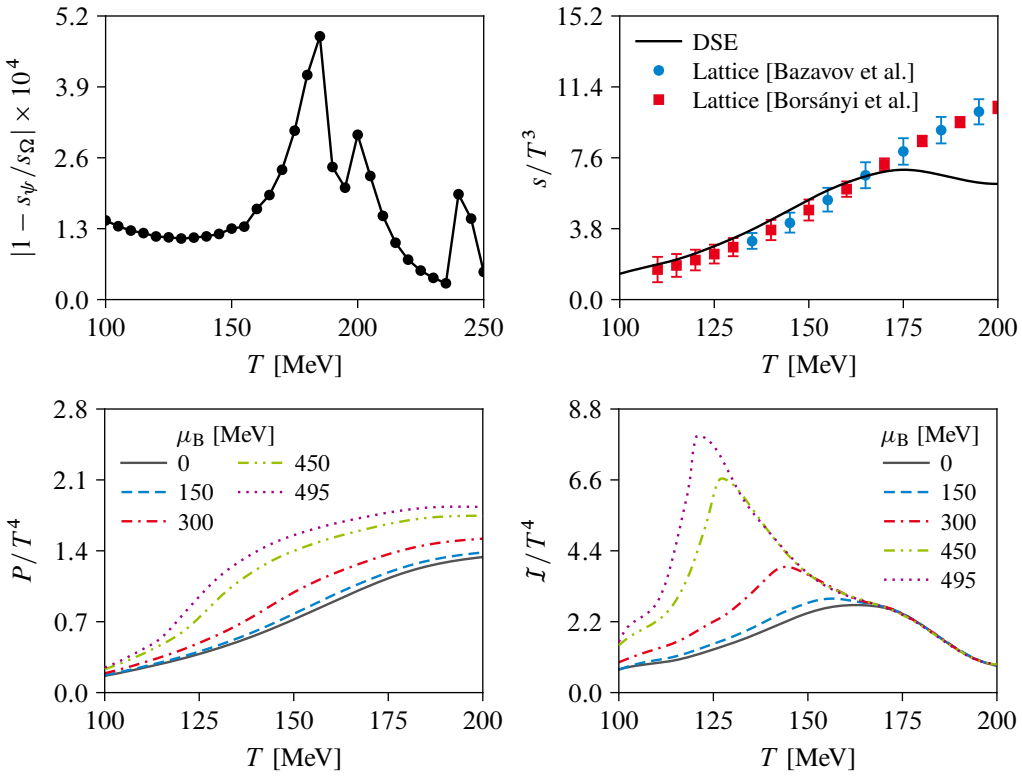

Figure 2: *Upper left:* relative error between the NJL entropy density obtained from the quark condensate through Eq. (4) (s_ψ) and directly from the thermodynamic potential (s_Ω). *Upper right:* entropy density at $\mu_B = 0$ in comparison to lattice results [4, 5]. *Lower left and right:* pressure and interaction measure, respectively, at different chemical potentials up to the CEP. All diagrams are adapted from Ref. [9].

4. Results and discussion

Proof of principle In order to demonstrate the viability of the method described in Sec. 2, we use a two-flavor Nambu–Jona-Lasinio (NJL) model in mean-field approximation [17]. It has the advantage that the thermodynamic potential can be computed explicitly and is given in a closed form. We are therefore in a position to compare the NJL entropy density obtained directly from the thermodynamic potential with the one resulting from Eq. (4).[2]

We find that both results cannot be distinguished by the eye, and the relative error between them is shown in the upper left diagram of Fig. 2: it is smaller than 0.05% across the whole temperature range. This shows that our method is reliable and works well.

EoS from DSEs Now, we summarize our thermodynamic results, which are discussed in detail in Ref. [9], obtained using the method described in Sec. 2 with quark-condensate data extracted from the DSE framework of Sec. 3.

Our result for the entropy density—the direct outcome of our method—at vanishing chemical potential is shown in the upper right diagram of Fig. 2 together with continuum-extrapolated lattice results [4, 5]. For $T \lesssim 170\,\text{MeV}$, it is monotonically increasing and, though with a slight overshoot,

[2] Here, $s_{\text{gauge}} = 0$ because gluons are no active d.o.f. in the NJL model.

in satisfying agreement with the lattice data. At higher temperatures, we observe an unphysical, nonmonotonous behavior. The reason for that can be traced back to our vertex ansatz: it overestimates the strength of the quark-gluon interaction at high temperatures and/or chemical potentials, which should become continuously weaker due to thermal screening. Addressing that issue is not the aim of this work, neither the delivery of a high-quality EoS; though we would like to note that our setup yields satisfying results in the temperature range 100–160 MeV, i.e., below and around the pseudocritical chiral transition temperature. More important, the key message is that the method of Sec. 2 allows us to obtain the entropy density from an elaborate DSE framework that does not admit an explicit calculation of the thermodynamic potential.

Having the entropy density $s(T,0)$ at vanishing chemical potential at hand, the pressure follows thermodynamically consistent from

$$P(T,\mu_\mathrm{B}) = P(T_0,0) + \int_{T_0}^{T} \mathrm{d}T'\, s(T',0) + \int_0^{\mu_\mathrm{B}} \mathrm{d}\mu'\, n(T,\mu')\,, \tag{5}$$

where the baryon number density $n(T,\mu_\mathrm{B})$ is calculated using the framework of Ref. [6], and $P(T_0,0)/T_0^4 = 0.242$ at $T_0 = 110\,\mathrm{MeV}$ [4]. Our results for the pressure at different chemical potentials ranging from zero to the CEP value $\mu_\mathrm{B}^\mathrm{CEP} = 495\,\mathrm{MeV}$ as functions of T are depicted in the lower left diagram of Fig. 2. The pressure gets larger with increasing chemical potential across the whole temperature range, although the increase is less noticeable at low temperatures. Its inflection point with temperature can be used to define the pseudocritical chiral transition temperature in the crossover region of the phase diagram and is compatible with other definitions like the peak position of the chiral susceptibility or the inflection point of the quark condensate. Approaching the CEP, a kink develops around the corresponding (chemical-potential dependent) pseudocritical chiral transition temperature, which is most pronounced close and at the CEP. Beyond that point, the pressure rises with a steep slope compared to low chemical potentials.

Since the entropy density is used to obtain the pressure, the latter inherits the erroneous high-temperature behavior from the former. This manifests in the fact that our results for the pressure saturate at too low temperatures and (well) below the Stefan–Boltzmann limit. However, the very same key message as stated above in case of the entropy density applies here.

Finally, our results for the interaction measure $\mathcal{I} = \varepsilon - 3P$ are shown in the lower right diagram of Fig. 2, where ε denotes the energy density, which is obtained by a Legendre transform of the pressure. At small chemical potentials, the interaction measure is shape consistent with lattice results and experiences as a function of temperature a strong increase from intermediate μ_B toward $\mu_\mathrm{B}^\mathrm{CEP}$. Close to and at the CEP, the slope becomes (near-)infinite at the corresponding critical temperature, and the peaklike structure with a large magnitude indicates that nonperturbative effects are manifest in this region of the QCD phase diagram.

Closing remarks We summarized a truncation-independent method to compute the EoS within nonperturbative functional approaches. At its heart lies an exact relation between the entropy density and the quark condensate. The method is particularly useful in the context of DSEs because it allows for the calculation of thermodynamic quantities within truncations that do not admit an explicit calculation of the thermodynamic potential—all current state-of-the-art DSE calculations [6–8, 10] are of that kind and future ones will certainly be like that, too.

Acknowledgments

This work was supported by HGS-HIRe for FAIR, the GSI Helmholtzzentrum für Schwerionenforschung, and the BMBF under contract 05P18RGFCA. We acknowledge computational resources provided by the HPC Core Facility and the HRZ of the Justus-Liebig-Universität Gießen.

References

[1] P. Braun-Munzinger and J. Wambach, *Colloquium: Phase diagram of strongly interacting matter*, *Rev. Mod. Phys.* **81** (2009) 1031 [0801.4256].

[2] B. Friman et al., eds., *The CBM Physics Book: Compressed Baryonic Matter in Laboratory Experiments*, no. 814 in Lecture Notes in Physics, Springer (2011).

[3] A. Bzdak et al., *Mapping the phases of quantum chromodynamics with beam energy scan*, *Phys. Rep.* **853** (2020) 1 [1906.00936].

[4] S. Borsányi et al., *Full result for the QCD equation of state with 2 + 1 flavors*, *Phys. Lett. B* **730** (2014) 99 [1309.5258].

[5] A. Bazavov et al., *Equation of state in (2 + 1)-flavor QCD*, *Phys. Rev. D* **90** (2014) 094503 [1407.6387].

[6] P. Isserstedt, M. Buballa, C.S. Fischer and P.J. Gunkel, *Baryon number fluctuations in the QCD phase diagram from Dyson–Schwinger equations*, *Phys. Rev. D* **100** (2019) 074011 [1906.11644].

[7] F. Gao and J.M. Pawlowski, *QCD phase structure from functional methods*, *Phys. Rev. D* **102** (2020) 034027 [2002.07500].

[8] F. Gao and J.M. Pawlowski, *Chiral phase structure and critical end point in QCD*, *Phys. Lett. B* **820** (2021) 136584 [2010.13705].

[9] P. Isserstedt, C.S. Fischer and T. Steinert, *Thermodynamics from the quark condensate*, *Phys. Rev. D* **103** (2021) 054012 [2012.04991].

[10] P.J. Gunkel and C.S. Fischer, *Locating the critical endpoint of QCD: Mesonic backcoupling effects*, *Phys. Rev. D* **104** (2021) 054022 [2106.08356].

[11] J. Bernhardt, C.S. Fischer, P. Isserstedt and B.-J. Schaefer, *Critical endpoint of QCD in a finite volume*, *Phys. Rev. D* **104** (2021) 074035 [2107.05504].

[12] J. Bernhardt, C.S. Fischer and P. Isserstedt, *Finite-volume effects in baryon number fluctuations around the QCD critical endpoint*, 2208.01981.

[13] C.S. Fischer, *QCD at finite temperature and chemical potential from Dyson–Schwinger equations*, *Prog. Part. Nucl. Phys.* **105** (2019) 1 [1810.12938].

[14] J.I. Kapusta and C. Gale, *Finite-Temperature Field Theory: Principles and Applications*, Cambridge University Press, 2nd ed. (2006).

[15] S. Borsányi et al., *Precision SU(3) lattice thermodynamics for a large temperature range*, *J. High Energy Phys.* **07** (2012) 056 [1204.6184].

[16] D. Binosi, J. Collins, C. Kaufhold and L. Theussl, *JaxoDraw: A graphical user interface for drawing Feynman diagrams. Version 2.0 release notes*, *Comput. Phys. Commun.* **180** (2009) 1709 [0811.4113].

[17] T. Hatsuda and T. Kunihiro, *QCD phenomenology based on a chiral effective Lagrangian*, *Phys. Rep.* **247** (1994) 221 [hep-ph/9401310].